Electronic structure and magnetic properties of rare-earth perovskite gallates from first principles

A Dahani[1,2], H Alamri[3], B Merabet[1,4,†], A Zaoui[1], S Kacimi[1], A Boukortt[5], and M Bejar[6]

[1] *Laboratoire de Physique Computationnelle des Matériaux, Université Djillali Liabès de Sidi Bel-Abbès, Sidi Bel-Abbès* 22000, *Algeria*
[2] *Université Moulay Tahar, Faculté de Technologie, Saida* 20000, *Algeria*
[3] *Umm Al-Qura University, Physics Department-University College, Makkah, Saudi Arabia*
[4] *Université Mustapha Stambouli, Faculté de Technologie, Mascara* 29000, *Algeria*
[5] *Elaboration Characterization Physico-Mechanics of Materials and Metallurgical Laboratory ECP3M, Faculty of Sciences and Technology, Abdelhamid Ibn Badis University of Mostaganem, Mostaganem* 27000, *Algeria*
[6] *Laboratoire de Physique Appliquée, Faculté des Sciences, Université de Sfax, Sfax* 3000, *Tunisia*

(Received 26 July 2016; revised manuscript received 28 September 2016; published online 30 November 2016)

The density functional calculation is performed for centrosymmetric (La–Pm) GaO_3 rare earth gallates, using a full potential linear augmented plane wave method with the LSDA and LSDA+U exchange correlation to treat highly correlated electrons due to the very localized 4f orbitals of rare earth elements, and explore the influence of $U = 0.478$ Ry on the magnetic phase stability and the densities of states. LSDA+U calculation shows that the ferromagnetic (FM) state of RGaO$_3$ is energetically more favorable than the anti-ferromagnetic (AFM) one, except for $LaGaO_3$ where the NM state is the lowest in energy. The energy band gaps of RGaO$_3$ are found to be in the range of 3.8–4.0 eV, indicating the semiconductor character with a large gap.

Keywords: DFT+U+SO, strongly correlated electron systems, magnetism, rare earth gallates perovskites

PACS: 71.27.+a, 71.15.Mb, 67.80.dk **DOI:** 10.1088/1674-1056/26/1/017101

1. Introduction

Recently, ABO_3 perovskites have become very attractive materials in many areas, due to their electrical properties such as piezoelectricity, pyroelectricity, ferroelectricity, and their thermal and chemical stability. The ABO_3 perovskites have been used in many applications:[1–7] capacitors, piezoelectric sonar, ultrasonic transducers, filters for radio and communication, pyroelectric surveillance systems, transducers for medical diagnostics, stereo speakers, lighters, ultrasonic motors, etc. The interest in ABO_3 perovskites is also caused by the ease of changing the nature of A and B cations in this structure and their valence state.[8,9] The change in these elements causes the appearance of new physical properties such as ferroelectricity ($BaTiO_3$), antiferroelectricity ($PbZrO_3$), magnetism ($LaMnO_3$, $La_{2/3}Sr_{1/3}MnO_3$), ferromagnetism ($YTiO_3$), antiferromagnetism ($LaTiO_3$), and superconductivity ($SrTiO_3$).[10,11]

The electronic structures of perovskites have been studied experimentally and theoretically for a very long time, such as the calculation of energy bands,[12] neutron diffraction and inelastic scattering data,[13] the photoemission spectra,[14] the optical spectra,[15] etc.

The orthorhombic perovskites, based on transition metals and rare earth elements RMnO$_3$, have been extensively studied. For example, Pimenov *et al.*[16] have synthesized $GdMnO_3$. Other compounds, such as RMnO$_3$[17–19] have been identified. Alonso *et al.* have determined the structural and magnetic properties of RNiO$_3$ (R = Sm, Eu, Gd, Dy, Ho, and Y) perovskites in the orthorhombic structure[20] using the x-ray diffraction. In 2002, Piamontese *et al.* presented the electronic and magnetic properties of perovskites-type RNiO$_3$ (R = Pr, Nd, Sm, Eu).[21]

In this work, we studied the magnetic stability and electronic structures of a series of ortho-rare earth gallates RGaO$_3$ (R = La, Ce, Pr, Nd, and Pm), that have been researched experimentally and theoretically, due to their technological interest. These materials have been analyzed by several research groups.[22–31] Theoretically, many calculations on the electronic structure were performed using different methods.[32–35] Our main goal is to achieve a better understanding of the electronic and magnetic properties of perovskites RGaO$_3$ (R = La, Ce, Pr, Nd, and Pm). On the other hand, we explain the R cation effect on different physical properties of these materials.

This paper is organized as follows: Section 2 gives a brief description of the calculation method. The predicted results are presented in Section 3 with a discussion. Finally, we give a summary in Section 4.

2. Calculation method

We performed our calculations within DFT implemented in the Wien2k code.[36] Atoms were represented by hybrid

†Corresponding author. E-mail: boualem19985@yahoo.fr

© 2017 Chinese Physical Society and IOP Publishing Ltd

full-potential linear augmented plane-wave plus local orbitals (L/APW+lo) method,[37] where wave functions, charge densities, and potentials were expanded in spherical harmonics within no overlapping muffin-tin (MT) spheres; plane waves were used in the remaining interstitial region of the unit cell. In the code, core and valence states were treated differently. Core states were treated within a multi-configuration relativistic Dirac–Fock approach, while valence states were treated in a scalar relativistic approach. The exchange–correlation energy was calculated using the Perdew–Wang local density approximation LSDA[38] and LSDA+U[39] (U: Hubbard parameter). To ensure the convergence of total energy in terms of the variational cutoff-energy parameter, a very careful step analysis was done. Then, we used an appropriate set of k-points to compute the total energy. We have computed equilibrium lattice constants and bulk moduli by fitting the total energy versus volume to the Murnaghan equation.[40] Standard built-in basis functions were applied with the valence configurations of (R : $5s^2 5p^6 4f^n 5d^1 6s^2$: $0 \le n \le 14$), (Ga: $3d^{10}4s^2 4p^1$) and (O: $2s^2 2p^3$). Total energy was minimized using a set of 36 k-points in the irreducible Brillouin zone for all studied structures, and a cutoff energy value of 8 Ry was used. Self-consistent calculations were considered to be converged only when the calculated total energy of the crystal converged to less than 1 mRy. The adopted MT radii were 2.5, 1.95, and 1.6 Bohr, respectively, for Ce, Ga, and O atoms.

We used the local spin-density approximation (LSDA)[38] to describe the exchange and correlation potentials. Since it is well known that such calculations cannot describe the strong on-site correlation between the 4f electrons, we added an effective Coulomb interaction $U_{\rm eff} = U$–J. The LSDA+U method essentially consists of identifying a set of atomic-like orbitals which were treated in a non-LSDA manner (with the standard double-counting correction[39]). Based on the lessons from Hubbard model studies, these orbitals are treated with an orbital-dependent potential with associated on-site Coulomb and exchange interactions U and J. The meaning of the U parameter was discussed by Anisimov and Gunnarsson,[41] who defined it as the cost in Coulomb energy by placing two electrons on the same site. In an atom, the U corresponds to F_0 of the unscreened Slater integrals.[41] Due to screening, the effective U in solids is much smaller than F_0 for atoms. The $U_{\rm eff}$ can be estimated by constraint DFT calculations, where some of the valence electrons are selectively treated as core electrons to switch off any hybridization with other electrons.[41] One can artificially simulate the addition and removal of electrons to the atomic shell and observe the change in the calculated total energy in order to estimate $U_{\rm eff}$. We constructed a supercell and proposed the hopping integrals connecting the 4f orbital of one atom. The number of electrons in this non-hybridizing f-shell was varied and $F^0_{\rm eff}$ was then calculated from

$$F^0_{\rm eff} = \varepsilon_{4f\uparrow}\left(\frac{n+1}{2}, \frac{n}{2}\right) - \varepsilon_{4f\uparrow}\left(\frac{n+1}{2}, \frac{n}{2}-1\right) - \varepsilon_{\rm F}\left(\frac{n+1}{2}, \frac{n}{2}\right) + \varepsilon_{\rm F}\left(\frac{n+1}{2}, \frac{n}{2}-1\right),$$

where $\varepsilon_{4f\uparrow}$ stands for the 4f spin-up eigenvalue of the rare earth atom. The original LSDA+U method[39] is based on the LMTO basis set, where the individual orbital and hopping terms can be identified; this is not possible within the LAPW method, so the method of Anisimov and Gunnarsson cannot be directly applied. Instead, the hybridization can be removed by putting the f states into the core or by performing a two-window calculation[42] and then U is calculated from $U - J = F^0_{\rm eff}$, where J can be calculated from the atomic values to a good approximation.

3. Results and discussion

3.1. Magnetic phase stability

In this part, we study the favorable magnetic configurations of these systems. For this, we prepared four possible independent spin configurations for our pérovskites RGaO$_3$ (R = Ce → Pm). Figure 1 shows the magnetic configurations considered in the ortho-rhombic structure, including the ferromagnetic state (FM), and the three antiferromagnetic phases AFM-(A, C, and G). Our purpose is to calculate the total energies of each magnetic configuration using the LSDA+U approach (U = 0.478 Ry[35]) to establish a comparison between the NM, FM, and AFM phases. Using the optimized atomic structure, orthorhombic *Pnma*, of RGaO$_3$ perovskites (R = Ce → Pm), total energies of all magnetic configurations, ferromagnetic (FM), and the three antiferromagnetic configurations were calculated according to the volumes by both LSDA and

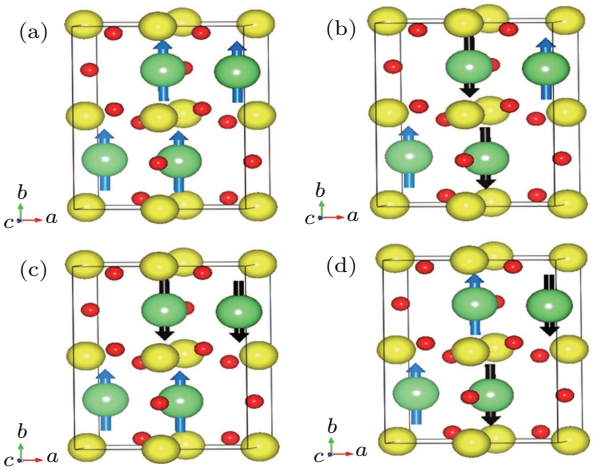


Fig. 1. (color online) Magnetic configurations in the orthorhombic structure, including: (a) ferromagnetic state (FM), and the three antiferromagnetic phases AFM-[(b) A, (c) C, and (d) G] using LSDA and LSDA+U.

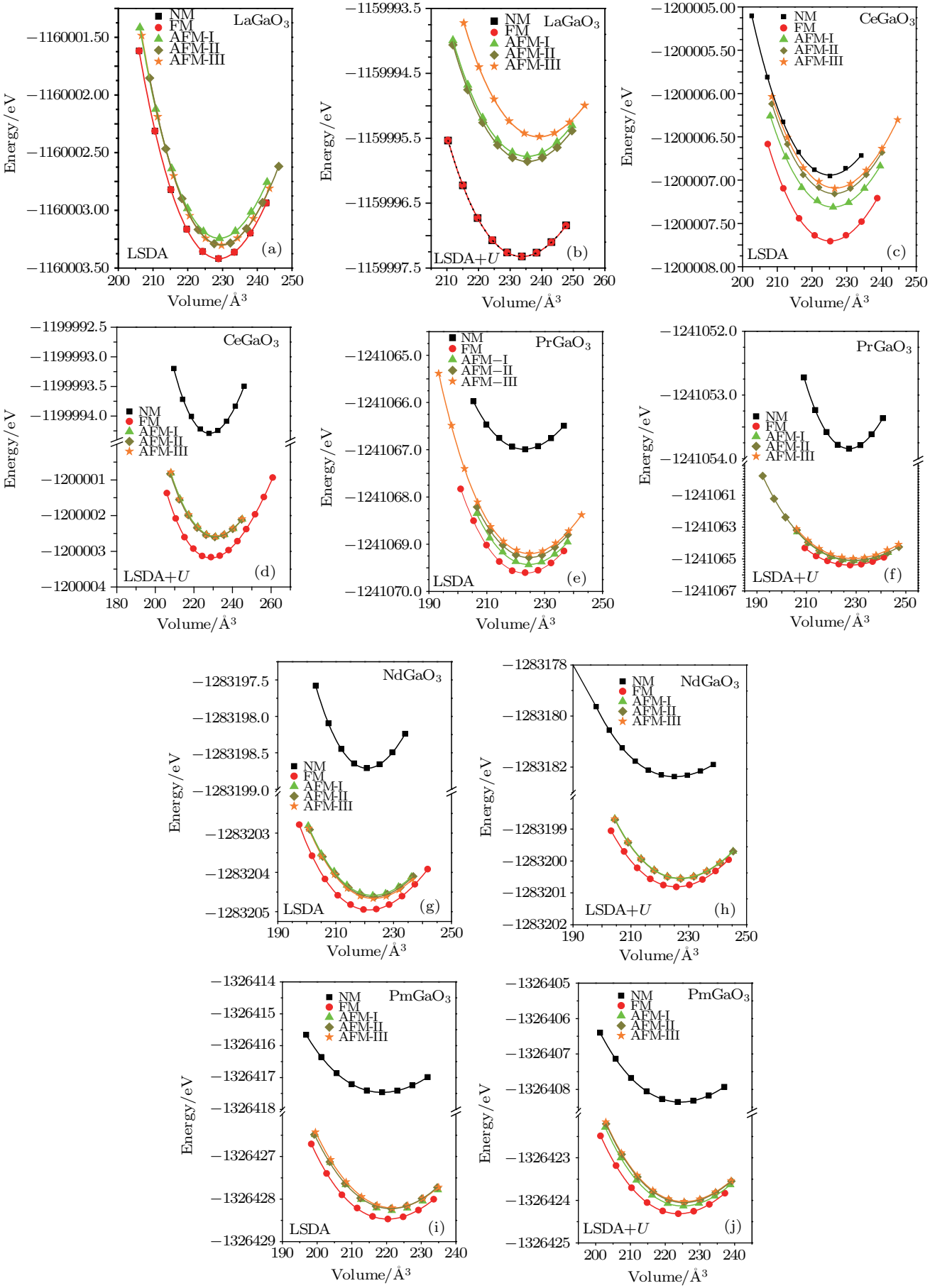


Fig. 2. (color online) Total energies of the tested magnetic: ferromagnetic (FM) and the three antiferromagnetic configurations calculated according to the volumes by LSDA (left column) and LSDA+U (right column). (a) and (b) $LaGaO_3$, (c) and (d) $CeGaO_3$, (e) and (f) $PrGaO_3$, (g) and (h) $NdGaO_3$, (i) and (j) $PmGaO_3$.

LSDA+U approximations, and are plotted in Fig. 2. It results that the non-magnetic (NM) state of the $LaGaO_3$ compound is the most stable compound using the LSDA+U approach, since the ground state energies of the two phases NM and FM (with and without polarized spin) are identical, as shown by the superposition of the two curves in Fig. 2. It is well known that standard approaches such as LSDA cannot describe the strong correlation between the 4f electrons, hence, it is necessary to include the effective coulomb interaction $U_{\text{eff}} = U - J$. The obtained results by both approaches clearly show that the FM configuration is the most stable compound for$R$GaO$_3$ compounds (R = Ce → Pm). Note that the obtained magnetic moment values are purely predictive.

3.2. Determination of structural parameters

Figure 3 shows the equilibrium lattice parameters a, b, and c of RGaO$_3$ (R = La→Pm) perovskites in the orthorhombic phase, calculated by LSDA and LSDA+U. Our results show that LSDA calculations underestimate the equilibrium volume V_0 and overestimate the bulk modulus B_0. From this figure, the variation of B_0 as a function of rare earth elements presents a strange behavior. We notice that the application of LSDA+U overestimates the lattice parameters compared with that obtained by LSDA, which is mainly due to the Hubbard repulsive potential U. We also note that the volume decreases along the series La→Pm, contrary to the bulk modulus that increases since it is inversely proportional to the lattice parameter. Hence, it is very clear that the LSDA+U approach provides results much better by comparing with the experimental data. LSDA calculations show that volumes differ from the experimental values of 3.18%, 3.25%, 3.25%, 3.96%, and 2.98%, respectively, for La→Pm, (see Table 1). The LSDA+U treatment of f localized electrons of our systems allows us to successfully reproduce all the structural properties (lattice parameters, bulk modulii, and internal parameters) by comparing with experimental values. Therefore, the main effect of the Hubbard correction is to prevent the participation of 4f electrons to the bonding: 4f states are pushed from the Fermi level towards lower and/or higher energies. Taking into account the correlations between the 4f electrons in the electronic structure of our perovskites, the LSDA+U approach shows a real improvement compared with all approximations based on the homogeneous electron gas. The experimental volume is well reproduced, like other properties related to the total energy as the bulk modulus. These first results, if they fail to be categorical about the behavior of 4f electrons of the ferromagnetic perovskites, indicate that at least part of them is localized.

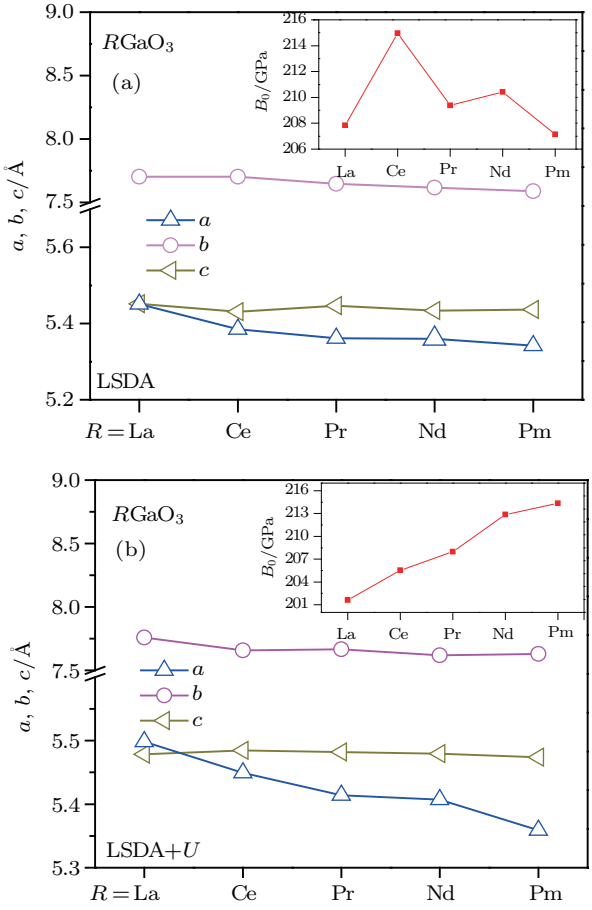


Fig. 3. (color online) Equilibrium lattice parameters a, b, and c of the FM perovskites RGaO$_3$ (R = La → Pm) in the orthorhombic phase calculated by LSDA (a) and LSDA+U (b).

Table 1. Volumes, lattice parameters a, b, and c, bulk moduli B, and their first derivatives for the ferromagnetic RGaO$_3$ compounds in the orthorhombic structure using LSDA and LSDA+U approaches and compared with other experimental results.

Compound	$LaGaO_3$		
E_{xc}	LSDA		
V/Å^3, a,b,c/Å	$V = 228.88$, $a = 5.451$, $b = 7.702$, $c = 5.450$		
B_0/GPa, B'	$B_0 = 208.83$ GPa, $B' = 4.3782$		
atomic site/Wyckoff multi-	x	y	z
La/4c	0.526967	0.25	0.493345
Ga/4b	0.5	0	0
O1/4c	0.989373	0.25	0.570139
O2/8d	0.779864	0.037245	0.220641
E_{xc}	LSDA+U/U = 0.478 Ry[35]		
V/Å^3, a,b,c/Å	$V = 233.70$, $a = 5.478$, $b = 7.757$, $c = 5.498$		
B_0/GPa, B'	$B_0 = 201.6260$, $B' = 4.4334$		
atomic site/Wyckoff mult-	x	y	z
La/4c	0.519784	0.25	0.497119
Ga/4b	0.5	0	0
O1/4c	0.994665	0.25	0.550894
O2/8d	0.775922	0.026756	0.224245

Table 1. (*Continued*).

Compound	$LaGaO_3$		
	experiment		
a,b,c/Å	$a = 5.524$,[43] $b = 7.774$,[43] $c = 5.492$[43]		
atomic site/Wyckoff mult-	x[43]	y[43]	z[43]
La/4c	−0.0041	0.0168	0.25
Ga/4b	0.5	0	0
O1/4c	0.0669	0.4942	0.25
O2/8d	−0.2701	0.2704	0.0356
	$V = 235.89$,[44] $a = 5.524$,[44] $b = 7.774$,[44] $c = 5.492$,[44]		
V/Å^3, a,b,c/Å	$V = 234.88$,[22] $a = 5.513$,[22] $b = 7.764$,[22] $c = 5.486$,[22]		
V/Å^3, B_0/GPa	$V = 235.1$,[45] $B_0 = 193.00$,[45] $B_0 = 208.00$,[45]		
a,b,c/Å	$a = 5.522$,[47] $b = 7.772$,[47] $c = 5.491$[47]		
atomic site/Wyckoff mult-	x[47]	y[47]	z[47]
La/4c	−0.0036	0.0172	0.25
Ga/4b	0.5	0	0
O1/4c	0.055	0.495	0.25
O2/8d	−0.72	0.281	0.029
	Theory		
V/Å^3, a,b,c/Å	$a = 5.465$,[48] $b = 7.737$,[48] $c = 5.56$[48]		

Compound	$CeGaO_3$		
E_{xc}	LSDA		
V/Å^3, a,b,c/Å	$V = 225.29$, $a = 5.431$, $b = 7.703$, $c = 5.384$		
B_0/GPa, B'	$B_0 = 214.97$, $B' = 4.1188$		
atomic site/Wyckoff mult-	x	y	z
Ce/4c	0.536938	0.25	0.490347
Ga/4b	0.5	0	0
O1/4c	0.986090	0.25	0.576397
O2/8d	0.786874	0.040302	0.213933
E_{xc}	LSDA+$U/U = 0.478$ Ry[35]		
V/Å^3, a,b,c/Å	$V = 228.84$, $a = 5.484$, $b = 7.656$, $c = 5.449$		
B_0/GPa, B'	$B_0 = 205.5269$, $B' = 4.8929$		
atomic site/Wyckoff mult-	x	y	z
Ce/4c	0.528176	0.25	0.493496
Ga/4b	0.5	0	0
O1/4c	0.986861	0.25	0.572666
O2/8d	0.774374	0.0397469	0.226000
	experiment		
V/Å^3, a,b,c/Å	$V = 233.24$,[49] $a = 5.484$,[49] $b = 7.747$,[49] $c = 5.490$[49]		
atomic site/Wyckoff mult-	x^{49}	y^{49}	z^{49}
Ce/4c	0.0276	0.25	0.9954
Ga/4b	0.5	0	0
O1/4c	0.4895	0.25	0.0889
O2/8d	0.2807	0.0318	0.7277
V/Å^3, a,b,c/Å	$V = 233.39$,[50] $a = 5.490$,[50] $b = 7.748$,[50] $c = 5.485$[50]		
atomic site/Wyckoff mult-	x[50]	y[50]	z[50]
Ce/4c	−0.0059	0.0276	0.25
Ga/4b	0.5	0	0
O1/4c	0.067	0.494	0.25
O2/8d	−0.289	0.275	0.07
V/Å^3, B_0/GPa	$V = 233.61$,[45] $B_0 = 177.00$,[45] $B_0 = 198.00$[45]		

Table 1. (*Continued*).

Compound	$PrGaO_3$		
E_{xc}	LSDA		
V/Å^3, a,b,c/Å	$V = 223.29$, $a = 5.446$, $b = 7.646$, $c = 5.361$		
B_0/GPa, B'	$B_0 = 209.3834$, $B' = 4.5635$		
atomic site/Wyckoff mult-	x	y	z
Pr/4c	0.542878	0.25	0.489765
Ga/4b	0.5	0	0
O1/4c	0.982514	0.25	0.579866
O2/8d	0.791401	0.042261	0.208937
E_{xc}	LSDA+U/U=0.478 Ryd[35]		
V/Å^3, a,b,c/Å	$V = 227.53$, $a = 5.482$, $b = 7.665$, $c = 5.414$		
B_0/GPa, B'	B_0= 204.9649, B'= 3.9714		
atomic site/Wyckoff mult-	x	y	z
Pr/4c	0.539468	0.25	0.490524
Ga/4b	0.5	0	0
O1/4c	0.984795	0.25	0.573871
O2/8d	0.785868	0.040409	0.214800
	experiment		
a,b,c/Å	$a = 5.455$,[51] $b = 7.727$,[51] $c = 5.490$[51]		
atomic site/Wyckoff mult-	x[51]	y[51]	z[51]
Pr/4c	−0.00742	0.03522	0.25
Ga/4b	0.5	0	0
O1/4c	0.0758	0.4848	0.25
O2/8d	−0.2868	0.2871	0.0404
V/Å^3, a,b,c/Å	$V = 230.72$,[22] $a = 5.449$,[22] $b = 7.710$,[22] $c = 5.493$[22]		
	$a = 5.462$,[51] $b = 7.740$,[51] $c = 5.493$[51]		
V/Å^3, B_0/GPa	$V = 231.4$,[45] $B_0 = 182.00$,[45] $B_0 = 220.00$[45]		
	theory		
V/Å^3, a,b,c/Å	$a = 5.401$,[48] $b = 7.669$,[48] $c = 5.557$[48]		

Compound	$NdGaO_3$		
E_{xc}	LSDA		
V/Å^3, a,b,c/Å	$V = 221.83$, $a = 5.433$, $b = 7.616$, $c = 5.360$		
B_0/GPa, B'	$B_0 = 210.4290$, $B' = 4.9390$		
atomic site/Wyckoff mult-	x	y	z
Nd/4c	0.542550	0.25	0.490296
Ga/4b	0.5	0	0
O1/4c	0.981360	0.25	0.580836
O2/8d	0.793412	0.042701	0.206972
E_{xc}	LSDA+U/U=0.478 Ryd[35]		
V/Å^3, a,b,c/Å	$V = 225.74$, $a = 5.479$, $b = 7.619$, $c = 5.407$		
B_0/GPa, B'	$B_0 = 212.8751$, $B' = 3.5546$		
atomic site/Wyckoff mult-	x	y	z
Nd/4c	0.543171	0.25	0.489357
Ga/4b	0.5	0	0
O1/4c	0.982900	0.25	0.578921
O2/8d	0.789498	0.042595	0.210862
	experiment		
a,b,c/Å	$a = 5.395$,[52] $b = 7.660$,[52] $c = 5.470$[52]		
atomic site/Wyckoff mult-	x[52]	y[52]	z[52]
Nd/4c	0.49089	0.04268	0.25
Ga/4b	0	0	0.5
O1/4c	0.7098	0.2092	0.5426
O2/8d	0.0803	0.0181	0.75
a,b,c/Å	$a = 5.405$,[52] $b = 7.679$,[52] $c = 5.475$[52]		
atomic site/Wyckoff mult-	x[52]	y[52]	z[52]
Nd/4c	0.49092	0.04142	0.25
Ga/4b	0	0	0.5
O1/4c	0.7107	0.2097	0.5422
O2/8d	0.0800	0.0174	0.75
a,b,c/Å	$a = 5.427$,[53] $b = 7.707$,[53] $c = 5.497$[53]		

Table 1. (*Continued*).

Compound	$NdGaO_3$		
atomic site/Wyckoff mult-	x[53]	y[53]	z[53]
Nd/4c	−0.0091	0.04142	0.25
Ga/4b	0.5	0	0
O1/4c	0.0800	0.4826	0.25
O2/8d	−0.2893	0.2903	0.0422
V/Å^3, a,b,c/Å	$V = 229.11$,[22] $a = 5.418$,[22] $b = 7.693$,[22] $c = 5.495$[22]		
	$a = 5.428$,[46] $b = 7.729$,[46] $c = 5.493$[46]		
V/Å^3, B_0/GPa	$V = 231.00$,[45] $B_0 = 189,00$,[45] $B_0 = 214,00$[45]		
	theory		
V/Å^3, a,b,c/Å	$a = 5.390$,[48] $b = 7.658$,[48] $c = 5.556$[48]		
$B_0 = 186,5$[54]			

Compound	$PmGaO_3$		
E_{xc}	LSDA		
V/Å^3, a,b,c/Å	$V = 220.30$, $a = 5.436$, $b = 7.588$, $c = 5.341$		
B_0/GPa, B'	$B_0 = 207.1398$, $B' = 4.9886$		
atomic site/Wyckoff mult-	x	y	z
Pm/4c	0.545001	0.25	0.489756
Ga/4b	0.5	0	0
O1/4c	0.980098	0.25	0.582616
O2/8d	0.796408	0.042915	0.203991
E_{xc}	LSDA+U/$U = 0.478$ Ry[35]		
V/Å^3, a,b,c/Å	$V = 223.77$, $a = 5.473$, $b = 7.628$, $c = 5.358$		
B_0/GPa, B'	$B_0 = 214.3356$, $B' = 4.4313$		
atomic site/Wyckoff mult-	x	y	z
Pm/4c	0.547594	0.25	0.489086
Ga/4b	0.5	0	0
O1/4c	0.979501	0.25	0.583705
O2/8d	0.792644	0.044405	0.207900
	experiment		
a,b,c/Å	$a = 5.396$,[55] $b = 7.677$,[55] $c = 5.507$[55]		
atomic site/Wyckoff mult-	x[55]	y[55]	z[55]
Pm/4c	−0.01121	0.04765	0.25
Ga/4b	0.5	0	0
O1/4c	0.08544	0.47598	0.25
O2/8d	−0.29291	0.28676	0.04473

Using the density functional theory, we have calculated electronic and magnetic properties of $RGaO_3$ perovskites (R = La → Pm) in the orthorhombic structure using LSDA and LSDA+U+SO approximations.

4. Partial and total densities of states

The calculated total (DOS) and partial (PDOS) densities of states with R-s/p/d/f, Ga-s/p/d, and O-s/p states for the $RGaO_3$ perovskites (R = La → Pm) are shown in Figs. 4 and 5. We note that LSDA gives a bad description of the Fermi area, which is largely dominated by the R-f localized states. Therefore, all our materials are found to be metallic except the NM-$LaGaO_3$ compound that has a semiconductor character using the three approaches (LSDA, LSDA+U, and LSDA+U+SO). Total densities of states plotted in Fig. 4, show a great topological similarity of the electrons distribution in conduction and valence regions. Therefore, the density of states can be divided into three regions separated by a gap. From the PDOS, we can identify the character of each region. The lower energies around −15 eV are derived from R-p, O-s, and Ga-d states, with a small contribution from Ga-s/p states in both spin directions (up and down). The second region from −8.0 eV to the Fermi energy (E_F) is derived from R-f states and O-p states of majority spin with a mixture of R-s/p/d, Ga-s/p/d, and Oxygen states. From ∼ 4 eV, the bands come from R-d/f with a mixture of Ga-s/p, R-s/p, and O-s/p states in both directions of the spin. Hence, it is very clear that the valence band maximum is mainly derived from R-f and O-p states with a small contribution of R-s/p states, while the conduction band minimum is dominated by R-d/f states with a small contribution of O-p and Ga-s/p states (see Fig. 5). When the spin–orbit interaction is taken into account (by the LSDA+U+SO approach), along the axis (001), the 4f orbitals are slightly modified; 4f spin states become larger and the energy shift between the centers becomes wider. The total magnetic moments of the unit cell of our materials, shown in Table 2, and are decomposed into atomic spheres contributions. For all approaches, the magnetic moments are strongly localized in the rare earth

element sites, with negligible contributions of gallium (Ga), oxygen (O) atoms and the interstitial region. We notice that using LSDA, LSDA+U, and LSDA+U+SO approaches, the calculated values of the magnetic moments are purely predictive. From Fig. 6, the magnetic moments increase from Ce ($4f^1$) toward Pm ($4f^4$) using these approximations.

Table 2. Total magnetic moments (μ_B) and band gap energies (E_g) for RGaO$_3$ perovskites (R = La → Pm) using different approximations.

	E_{xc}	$(M/R)/\mu_B$	$(M/T)/\mu_B$	Direction	E_g/eV	
LaGaO$_3$	LDA	–	–	$T \to \Gamma$	$E_g = 3.94923$	
	LDA+U	–	–	$T \to \Gamma$	$E_g = 3.68888$	
	LDA+U+SO	–	–	$T \to \Gamma$	$E_g = 3.68726$	
CeGaO$_3$	LDA	0.9593	3.9906	–	–	–
	LDA+U	0.9854	4.0041	$T \to \Gamma$	$E_g \uparrow = 3.81529$	$E_g \downarrow = 3.83622$
	LDA+U+SO	0.9877	3.9999	$T \to \Gamma$	$E_g \uparrow = 3.81341$	$E_g \uparrow$=3.69803
PrGaO$_3$	LDA	1.9715	7.9879	–	–	–
	LDA+U	1.9866	8.0007	$T \to \Gamma$	$E_g \uparrow = 3.8942$	$E_g \downarrow = 3.94676$
	LDA+U+SO	1.9853	7.9981	$T \to \Gamma$	$E_g \uparrow = 3.84168$	$E_g \downarrow = 3.88137$
NdGaO$_3$	LDA	3.0006	12.0035	–	–	–
	LDA+U	2.9926	11.9987	$T \to \Gamma$	$E_g \uparrow = 3.96875$	$E_g \downarrow = 4.01297$
	LDA+U+SO	2.9878	11.9930	$T \to \Gamma$	$E_g \uparrow = 3.93188$	$E_g \downarrow = 3.95254$
PmGaO$_3$	LDA	4.0427	16.0412	–	–	–
	LDA+U	3.9986	16.0006	$T \to \Gamma$	$E_g \uparrow = 4.023$	$E_g \downarrow = 4.06848$
	LDA+U+SO	3.9941	15.9942	$T \to \Gamma$	$E_g \uparrow = 4.01265$	$E_g \downarrow = 4.17249$

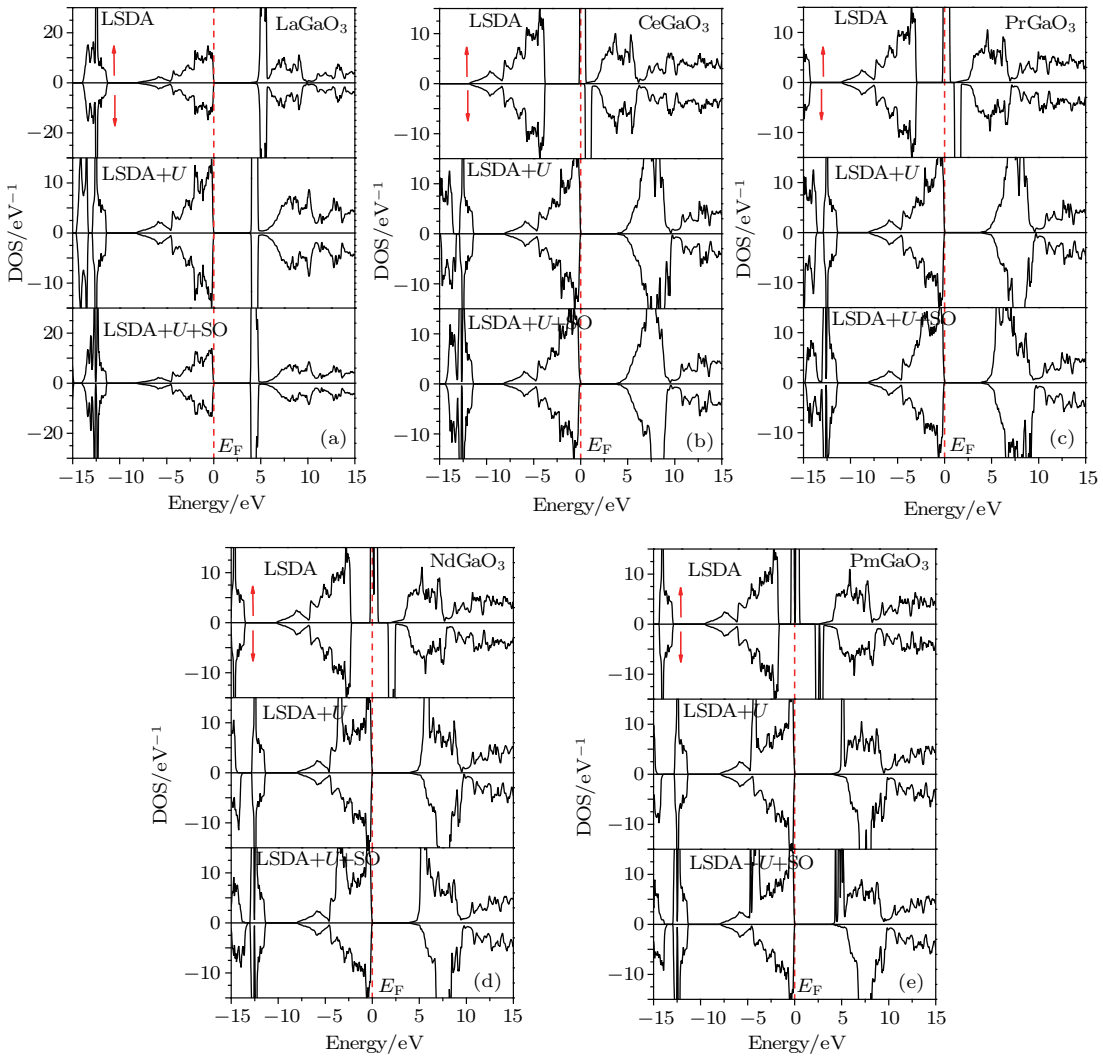


Fig. 4. (color online) Calculated total densities of states (DOS) for RGaO$_3$ perovskites (R = La → Pm) using LSDA, LSDA+U, and LSDA+U+SO: (a) LaGaO$_3$, (b) CeGaO$_3$, (c) PrGaO$_3$, (d) NdGaO$_3$, and (e) PmGaO$_3$.

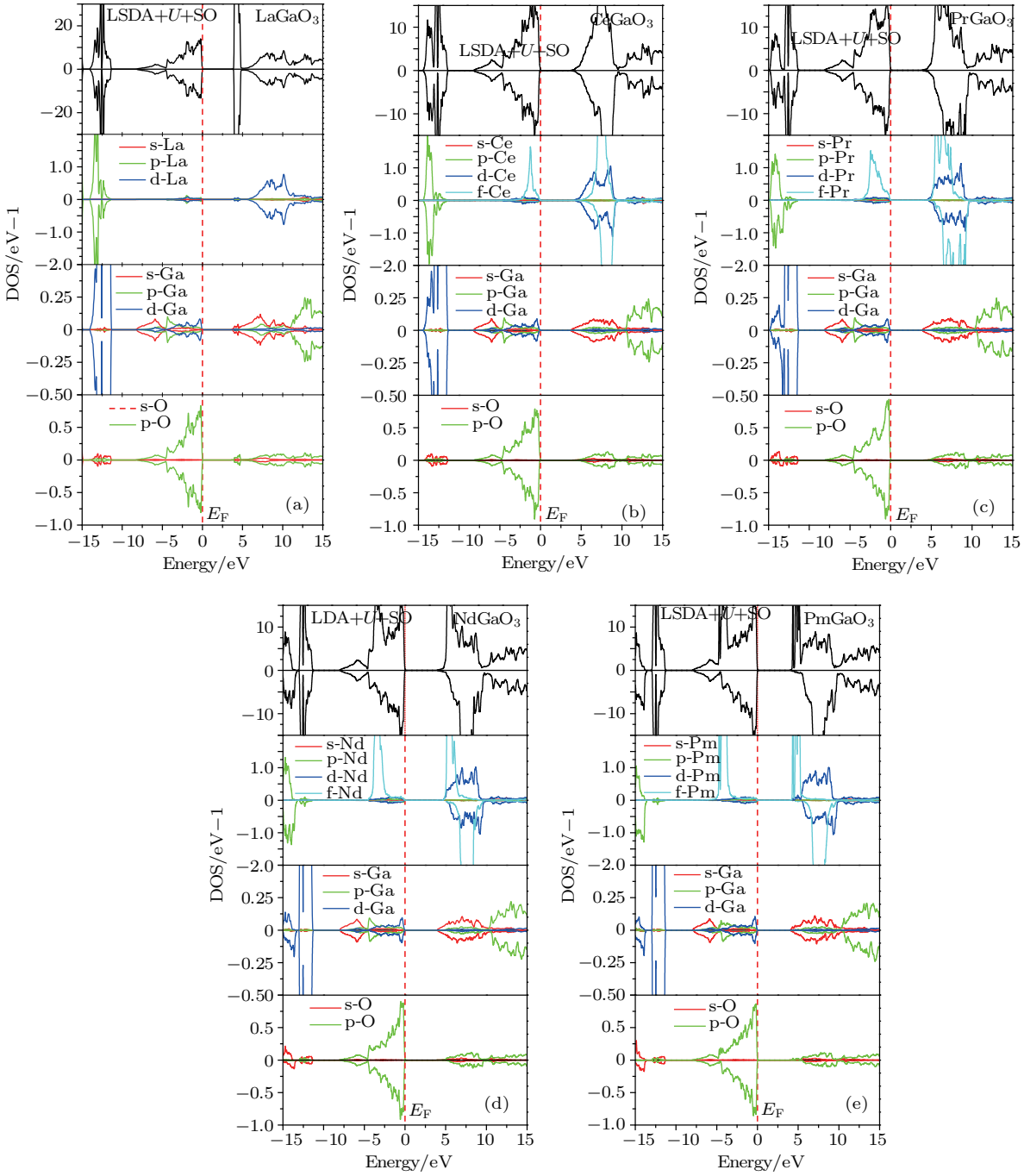


Fig. 5. (color online) Calculated partial densities of states (PDOS), using LSDA+U+SO, with R-s/p/d/f, Ga-s/p/d and O-s/p, for $RGaO_3$ perovskites (R = La → Pm): (a) $LaGaO_3$, (b) $CeGaO_3$, (c) $PrGaO_3$, (d) $NdGaO_3$, and (e) $PmGaO_3$.

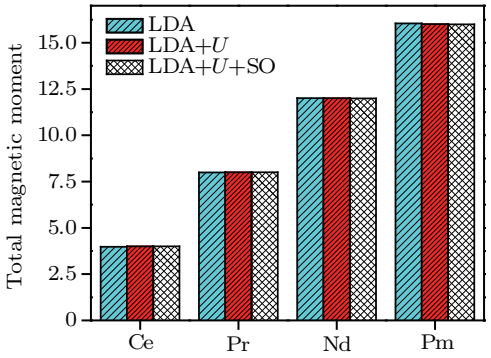


Fig. 6. (color online) Calculated values of the magnetic moments of (Ce, Pr, Nd, and Pm) rare earth elements using LSDA, LSDA+U, and LSDA+U+SO.

5. Electronic charge density

In this part, we calculated the distribution of the valence charge density of the orthorhombic $RGaO_3$ (R = La → Pm) perovskites in the (100) plane succeeding in both spin directions and by using LSDA+U+SO. Due to the similarity of the charge density results of the studied systems, we presented only the charge and spin densities of the $CeGaO_3$ compound, as shown in Fig. 7(a). There is a charge transfer from metallic atoms (R and Ga) to the nonmetallic one, since the oxygen is more electronegative than these elements. This charge transfer between the cation and anion increases with the electronega-

tivity difference increasing. It may be noted that there is an increase in the electronic charge distribution in the O sites, while it decreases in *R* and Ga sites. This charge rearrangement reflects the electronegative nature of O and explains the ionicity of the bonding. The charge density shown in Fig. 7(a) indicates the predominant covalent character of the established chemical bonding between the O atom and that of Ga, accompanied by a charge transfer from Ga toward the nonmetallic atom, which means a degree of ionicity in the bonding. This is due to the hybridization effect between the Ga-d states and O-p states. The *R*–O bonding in $RGaO_3$ perovskites seems to have an ionic character. Figure 7(b) shows the spin density (difference between spin-up and spin-down electron densities) in a plane perpendicular to the axis of symmetry containing *R*, Ga, and O atoms. The spin density of gallium and oxygen in the spin density vicinity of rare earth atoms is of the opposite sign (not shown in Table 2). From this figure, it becomes clear why the magnetic moments of atoms are negligible and negative and the origin of magnetism comes from the rare earth element *R*, since the spin density has a spin magnetic moment mainly due to 4f orbitals.

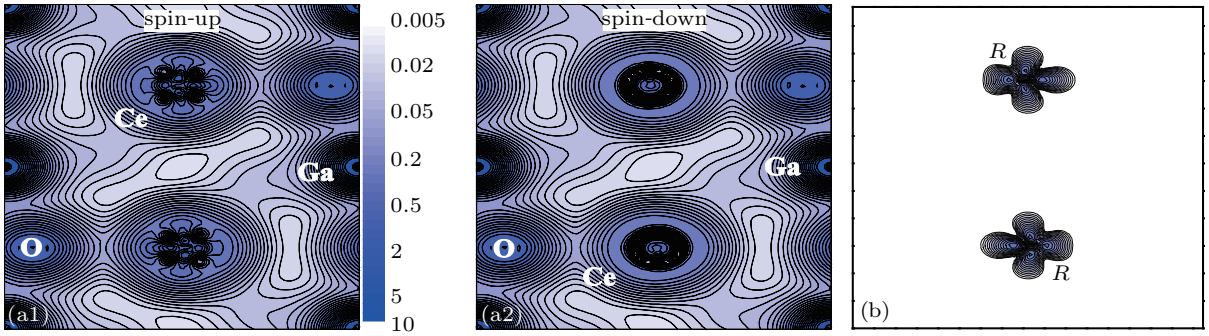


Fig. 7. (color online) (a) Charge density of the $CeGaO_3$ compound, (b) spin density of $CeGaO_3$, in a plane perpendicular to the axis of symmetry containing *R*, Ga, and O atoms using LSDA+*U*+SO.

6. Conclusion

To conclude, no *ab-initio* calculations at present, to the best of our knowledge, have allowed the study and exploitation of the electronic and magnetic properties of $RGaO_3$ perovskites. Therefore, it would be worth taking into consideration the strongly correlated 4f electrons using the LSDA+*U* approach. The application of this approximation led to two major advances. (i) The experimental volume is reproduced as well as other properties related to the total energy like the bulk modulus. (ii) The LSDA+*U* approach shows that $RGaO_3$ perovskites are indirect gap ($T \rightarrow \Gamma$) insulators with values in the range of $\sim (3.68, 4.00)$ eV. Using both LSDA and LSDA+*U* approaches, the calculated magnetic moments are purely predictive. Spin–orbit coupling is taken into account to better treat 4f-*R* bands. Experimental investigations should be quite interesting. The theory efficiency in research of the ground state is again demonstrated, so the calculation tool used in this work is helpful to predict new structural, electronic, and magnetic properties, which exhibit a significant contribution in several application fields.

References

[1] Zhou D, Chen Y, Zhang D, Liu H, Hu Y and Gong S 2004 *Sensor Actuat. A* **116** 450
[2] Benziada-Taïbi L 2005 *Mater. Sci. Forum* **492–493** 114
[3] Hu T, Uusimäki A, Jantunen H, Leppävuori, Soponmanee K S and Sirisoonthorn S 2005 *Ceram. Int.* **31** 85
[4] Lee B D, Lee H R, Yoon K H and Cho Y S 2005 *Ceram. Int.* **31** 143
[5] Cho W W, Ohsato H and Zouganelis G 2006 *J. Eur. Ceram. Soc.* **26** 1865
[6] Kumagai S, Wakino K, Ando A and Kitazawa T 2006 *J. Eur. Ceram. Soc.* **26** 1817
[7] Wang S, Zhang S, Zhou X, Li B and Chen Z 2006 *Mater. Lett.* **60** 909
[8] Pe na M A and Fierro J L G 2001 *Chem. Rev.* **101** 7
[9] Russo N, Fino D, Saracco G and Specchia V 2005 *J. Catal.* **229** 459
[10] Smyth D M 1985 *Ann. Rev. Mater. Sci.* **15** 329
[11] Tsuda N, Nasu K, Fujimori A and Siratori K 2000 *Electronic Conduction in Oxides* (2nd edn.) (Berlin: Springer-Verlag) p. 365
[12] Mattheiss L F 1972 *Phys. Rev. B* **6** 4718
[13] Wqllan E O and Kqehler W C 1955 *Phys. Rev. Lett.* **100** 2
[14] Battye F L, Höchst H and Goldmann A 1976 *Solid State Commun.* **19** 269
[15] Lightsey P A 1973 *Phys. Rev. B* **8** 3586
[16] Pimenov A, Mukhin A A, Ivanov V Y, Travkin V D, Balbashov A M and Loidl A 2006 *Nature Phys.* **2** 97
[17] Senff D, Link P, Hradil K, Hiess A, Regnault L P, Sidis Y, Aliouane N and Argyriou D N 2007 *Phys. Rev. Lett.* **98** 137206
[18] Aguilar R V, Sushkov A B, Zhang G L, Choi Y J, Cheong S W and Drew H D 2007 *Phys. Rev. B* **76** 060404
[19] Pimenov A, Shuvaev A M, Mukhin A A and Loidl A 2008 *J. Phys.: Condens. Matter* **20** 434209
[20] Alonso J A, Martinez-Lope M J, Casais M T, Aranda M A G and Fernandez-Diaz M T 1999 *Am. Chem. Soc.* **121** 4754
[21] Piamonteze C, Tolentino H C N, Ramos A Y, Massa N E, Alonso J A, Martinez-Lope M J and Casais M T 2002 *Physica B* **320** 71
[22] Senyshyn A, Trots D M, Engel J M, Vasylechko L, Ehrenberg H, Hansen T, Berkowski M and Fuess H 2009 *J. Phys.: Condens. Matter* **21** 145405
[23] Parveen A and Gaur N K 2012 *Solid State Sci.* **14** 814
[24] Glowacki M, Runka T, Domukhovski V, Diduszko R, Mirkowska M, Berkowski M and Dabrowski B 2011 *J. Alloys Compd.* **509** 1756
[25] Ishihara T, Eto H and Yan J W 2011 *J. Hydrogen Energy* **36** 1862
[26] Vasylechko L, Pivak Y, Senyshyn A, Savytskii D, Berkowski M, Borrmann H, Knapp M, and Paulmann C 2005 *J. Solid State Chem.* **178** 270
[27] Senyshyn A, Schnelle W, Vasylechko L, Ehrenberg H and Berkowski M 2007 *J. Phys.: Condens. Matter* **19** 156214
[28] Parveen A, Srivastava A and Gaur N K 2011 *Am. Inst. Phys.* **1393** 291
[29] Mathews M, Houwman E P, Boschker H, Rijnders G and Blank D H A 2010 *J. Appl. Phys.* **107** 013904

[30] Reshak A H, Piasecki M, Auluck S, Kityk I V, Khenata R, Andriyevsky B, Cobet C, Esser N, Majchrowski A, Świrkowicz M, Diduszko R and Szyrski W 2009 *J. Phys. Chem. B* **113** 15237
[31] Piasecki M, Andriyevsky B, Cobet C, Esser N, Kityk I V, Świrkowicz M and Majchrowski A 2010 *Opt. Commun.* **283** 3998
[32] Senyshyn A, Ehrenberg H, Vasylechko L, Gale J D and Bismayer U 2005 *J. Phys.: Condens. Matter* **17** 6217
[33] T Tohei, Moriwake H, Murata H, Kuwabara A, Hashimoto R, Yamamoto T and Tanaka I 2009 *Phys. Rev. B* **79** 144125
[34] Novak P, Knizek K, Marysko M, Jirak Z and Kune J 2013 *Phys. Rev. B* **87** 205139
[35] Hasni W, Boukortt A, Bekkouche B, Kacimi S, Djermouni M and Zaoui A 2012 *Physica B* **407** 901
[36] Blaha P, Schwarz K, Madsen G K H, Kvasnicka D and Luitz J 2001 *Wien2K, An Augmented Plane Wave Plus Local Orbitals Program For Calculating Crystal Properties, Vienna University of Technology, Vienna*
[37] Sjöstedt E, Nordstrom L and Singh D J 2000 *Solid State Commun.* **114** 15
[38] Perdew J P and Wang Y 1992 *Phys. Rev. B* **45** 13244
[39] Anisimov V I and Gunnarsson O 1991 *Phys. Rev. B* **43** 7570
[40] Murnaghan F D 1944 *Proc. Natl. Acad. Sci. USA* **30** 5390
[41] Anismov V I and Gunnarsson O 1991 *Phys. Rev. B* **43** 7570
[42] Madsen G K H and Nova'k P 2005 *Eur. Phys. Lett.* **69** 777
[43] Howard C J and Kennedy B J 1999 *J. Phys: Condens. Matter* **11** 3229
[44] Kajitani M, Matsuda M, Hoshikawa A, Oikawa K I, Torii S, Kamiyama T, Izumi F and Miyake M 2003 *Chem. Mater.* **15** 3468
[45] Senyshyn A, Engel J M, Oswald I D H, Vasylechko L, Berkowski M 2009 *Z. Kristallogr. Suppl.* **30** 341
[46] Parveen A, Srivastava A and Gaur N K 2011 *Solid State Phys.* **1349** 975
[47] Vasylechko L, Matkovski A, Suchocki A, Savytskii D and Syvorotka I 1999 *J. Alloys Compd.* **286** 213
[48] Ubic R and Subodh G 2009 *J. Alloys Compd.* **488** 374
[49] Stan M, Armstrong T J, Butt D P, Wallace T C S, Park Y S, Haertling C L, Hartmann T and Hanrahan R J J 2002 *J. Am. Ceram. Soc.* **85** 2811
[50] Vasylechko L O, Niewa R, Senyshyn A T, Pivak Y, Savytskii D, Knapp M and Bähtz C 2002 *Hasylab. Ann. Rep.* **1** 223
[51] Sasaura M, Mukaida M and Miyazawa S 1990 *Appl. Phys. Lett.* **57** 2728
[52] Vasylechko L, Akselrud L, Morgenroth W, Bismayer U, Matkovskii A and Savytskii D 2000 *J. Alloys Compd.* **297** 46
[53] Piasecki M, Andriyevsky B, Cobet C, Esser N, Kityk I V, Świrkowicz M and Majchrowski A 2010 *Opt. Commun.* **283** 3998
[54] Senyshyn A, Vasylechko L, Knapp M, Bismayer U, Berkowski M and Matkovskii A 2004 *J. Alloys Compd.* **382** 84
[55] Senyshyn A, Ehrenberg H, Vasylechko L, Gale J D and Bismayer U 2005 *J. Phys.: Condens. Matter* **17** 6217